Environmental Science
Processes & Impacts

Evaluation of iodide chemical ionization mass spectrometry for gas and aerosol-phase per- and polyfluoroalkyl substances (PFAS) analysis

Journal:	*Environmental Science: Processes & Impacts*
Manuscript ID	EM-ART-06-2022-000275.R2
Article Type:	Paper

Environmental Significance Statement for:

Evaluation of iodide chemical ionization mass spectrometry for gas and aerosol-phase per- and polyfluoroalkyl substances (PFAS) analysis

Bailey B. Bowers,[1] Joel A. Thornton,[2] Ryan C. Sullivan[1,3*]

[1] Department of Chemistry, Carnegie Mellon University, Pittsburgh, PA, USA

[2] Department of Atmospheric Sciences, University of Washington, Seattle, WA

[3] Department of Mechanical Engineering, Carnegie Mellon University, Pittsburgh, PA, USA

* Corresponding author: rsullivan@cmu.edu

Environmental Significance Statement

Per- and polyfluoroalkyl substances (PFAS) are ubiquitous in the atmosphere, but our understanding of the time-resolved behavior of PFAS in the gas and aerosol phase is limited by currently available methodology. Online methods such as iodide-time-of-flight chemical ionization mass spectrometry (iodide-ToF-CIMS) would be a valuable addition to understand the atmospheric behavior of PFAS. While iodide-ToF-CIMS has been previously used to characterize a few PFAS, we expand the classes of PFAS that can be analyzed by this method and improve understanding of how iodide reagent ions interact with these analytes. Together, these findings enable online measurements of PFAS in gas and aerosol phases, improving understanding of the atmospheric fate and transport of these ubiquitous, persistent, and toxic contaminants in the environment.

Evaluation of iodide chemical ionization mass spectrometry for gas and aerosol-phase per- and polyfluoroalkyl substances (PFAS) analysis

Bailey B. Bowers,[1] Joel A. Thornton,[2] Ryan C. Sullivan[1,3*]

[1] Department of Chemistry, Carnegie Mellon University, Pittsburgh, PA, USA

[2] Department of Atmospheric Sciences, University of Washington, Seattle, WA

[3] Department of Mechanical Engineering, Carnegie Mellon University, Pittsburgh, PA, USA

* Corresponding author: rsullivan@cmu.edu

Abstract

Per- and polyfluoroalkyl substances (PFAS) are a class of ultra-persistent anthropogenic contaminants. PFAS are ubiquitous in environmental and built systems, but very few online methods exist for their characterization in atmospheric gases and aerosols. Iodide time-of-flight chemical ionization mass spectrometry (iodide-ToF-CIMS) is a promising technology for online characterization of PFAS in the atmosphere. Previous work using iodide-ToF-CIMS was successful in measuring gas-phase perfluoroalkyl carboxylic acids and fluorotelomer alcohols, but those are just two of the myriad classes of PFAS that are atmospherically relevant. Therefore, our first objective was to test other sample introduction methods coupled to iodide-TOF-CIMS to evaluate its ability to measure a wider suite of PFAS in both gas and aerosol phases. Using a variety of sample introduction techniques, we successfully measured gas-phase fluorotelomer alcohols (FTOHs), gas and aerosol-phase perfluoroalkyl carboxylic acids (PFCAs), and aerosol-phase perfluoroalkyl sulfonic acids and polyfluoroalkyl phosphoric acid diesters (PFSAs and diPAPs). We also determined iodide-ToF-CIMS response factors for these compounds by introducing known quantities using a Filter Inlet for Gases and AEROsols (FIGAERO). These response factors ranged from 400 to $6x10^4$ ions per nanogram, demonstrating low limits of detection. Furthermore, PFAS are a poorly understood diverse class of molecules that exhibit unusual and often unexpected physicochemical properties due to their highly fluorinated nature. Since detection of PFAS with iodide-ToF-CIMS relies on the analyte molecule to either undergo proton transfer or adduct formation with iodide, understanding PFAS behavior during chemical ionization gives rise to a more fundamental understanding of these compounds. Through voltage scanning experiments and DFT calculations, we found that PFCAs and FTOHs readily form iodide adducts, while PFSAs and diPAPs preferentially undergo proton transfer to iodide. Generally, binding energy increased

with increasing linear chain length, and PFCAs had stronger binding than FTOHs. Overall, our results suggest that iodide-ToF-CIMS can be used to measure even nonvolatile PFAS such as PFSAs and diPAPs in the aerosol phase in a semi-continuous online fashion.

Introduction

Per- and polyfluoroalkyl substances (PFAS) are a class of anthropogenic contaminants, some of which are toxic. [1] Due to their high persistence and/or high persistence of their transformation products, PFAS are ubiquitous in natural and built environments.[2] The presence of some PFAS (especially perfluoroalkyl carboxylic acids, or PFCAs and perfluoroalkyl sulfonic acids, or PFSAs)in surface water, drinking water, groundwater, arctic ice, soil, and human blood serum is well characterized due to robust analytical techniques for these matrices.[2] However, few techniques can measure PFAS in atmospheric systems, meaning that gas and aerosol phase PFAS are not well characterized. Manufacturing, use, and disposal of products containing PFAS result in emission of these compounds to indoor and outdoor air.[3–12] Due to the lack of appropriate analytical techniques, these emissions are often not directly measured, and instead are characterized by the downstream deposition of these compounds or their transformation products (which are often still highly fluorinated) to soil, water, dust, or ice.[13–17] When PFAS are directly measured in the gas or aerosol phase, they are measured in an offline mode, by either passive or active sampling onto media, followed by extraction and analysis via LC-MS or GC-MS.[4,7–12] Offline measurements lack temporal resolution, and sample collection and preparation can introduce contamination and other biases or artefacts.[18,19]

Many PFAS are of atmospheric relevance, even though the few available gas and aerosol-phase measurement methods precludes a thorough understanding of PFAS in the atmosphere, especially for newer PFAS more recently brought into production that lead to new emerging contaminants. Neutral PFAS such as fluorotelomer alcohols (FTOH), perfluorooctane sulfonamides (FOSA), perfluorooctane sulfonamidoethanols (FOSE) are quite volatile relative to other PFAS, so their presence in the gas phase is expected and widely observed.[11,20,21] Neutral PFAS are often referred to as perfluoroalkyl acid precursors, since oxidation can transform these compounds into perfluoroalkyl carboxylic acids (PFCAs) or perfluoroalkyl sulfonic acids (PFSAs).[22–25] Since PFCAs and PFSAs are less volatile and often ionic, they are typically found in the condensed phase. PFCAs and PFSAs have been measured in atmospheric particulate matter and sea spray aerosols.[12,26,27] The latter is likely due to the high surface activity of these compounds, meaning

their concentrations are enhanced at the air-water interface. Finally, many of the aforementioned PFAS, as well as polyfluoroalkyl phosphoric acid diesters (diPAPs), perfluorophosphonates (PFPAs), and perfluorophosphinates (PFPIAs), have been measured in indoor dust.[16,17,28–32] diPAPs have been shown to also be PFAA precursors, as atmospheric photooxidation on mineral dust can transform these compounds to PFCAs.[33]

Given the wide variety of PFAS present in the atmosphere, as well as the limitations of offline methods, an online method for PFAS monitoring in gases and aerosols would be highly valuable for better characterization of atmospheric inputs, fluxes, transport, and transformations of PFAS. Time-of-flight chemical ionization mass spectrometry (ToF-CIMS) is well-suited to this objective, since it enables measurements at high time resolution (1 Hz) and can achieve sub-pptv detection limits.[34] Furthermore, CIMS utilizes a soft ionization technique, meaning minimal fragmentation occurs in the ion source, preserving the original molecular identity. When coupled with a high mass resolution (>10,000) time-of-flight mass spectrometer, this allows for molecular formula assignment of unknown species, otherwise known as nontarget analysis. Nontarget analysis is especially valuable for PFAS research, as manufacturers continually introduce new PFAS without disclosure of their molecular formulae or structures.[13,35–40]

Another benefit of CIMS is its high selectivity, which can be tuned with the choice of reagent ion. Iodide is an especially attractive reagent ion for PFAS since it is a very weak gas-phase base (meaning it tends to form adducts with analytes rather than abstracting a proton). The large mass defect and large atomic mass of iodide makes it easy to identify ions that are iodide-containing clusters produce by the chemical ionization.[34] There is also recent precedent for measuring PFAS via iodide ToF-CIMS. Riedel et al. demonstrated that this a reliable technique to measure perfluoroalkyl carboxylic acids (PFCAs) and fluorotelomer carboxylic acids (FTOH) in the gas phase, with low (on the order of pptv) limits of detection.[41]

However, due to the sample introduction technique used (humidified clean air), Riedel et al. were only able to detect volatile and semivolatile PFAS, meaning the widely used perfluoroalkyl sulfonic acids (PFSAs) or polyfluoroalkyl phosphoric acid diesters (diPAPs) were not detected with this method. Therefore, our first objective was to test other sample introduction methods coupled to I-CIMS to evaluate their ability to measure a wider suite of PFAS in both gas and aerosol phases. We investigated three sample introduction methods: The first method generates aqueous aerosol droplets containing PFAS. This aerosol was then passed through a heated tube, to

generate gas-phase PFAS through solvent evaporation. We refer to this as the "heated tube" method.

The second method, suitable for neutral, volatile PFAS, involved simply passing a flow of nitrogen gas through the headspace of a glass bulb containing liquid PFAS or a PFAS solution. We refer to as the "diffusion tube" method. The third method employed a Filter Inlet for Gases and AEROsols (FIGAERO), which is specialized inlet designed for use with the iodide ToF-CIMS. The FIGAERO is described in detail elsewhere.[42] Briefly, the inlet contains an actuator, which holds a Teflon filter. This Teflon filter allows for sampling of aerosol particles, while the ToF-CIMS analyzes the gas phase. Then, after adequate particulate matter has been sampled onto the filter, the actuator is moved so the gas-phase sampling is blocked, and the filter is moved directly upstream of the instrument's orifice. Heated nitrogen flow desorbs the material on the filter, creating gas-phase analyte molecules. For the purpose of this study, solutions of PFAS were intentionally spotted onto the Teflon filter and desorbed to generate signal. FIGAERO was also used to calibrate the instrument response to PFCAs, PFSAs, and diPAPs. By spotting known quantities of these compounds onto the Teflon filter and desorbing it, we determine the response factor in terms of ions per nanogram. This approach has been previously employed by groups using iodide-CIMS to study secondary organic aerosol.[43,44]

Furthermore, despite their ubiquity, PFAS are not well understood, as the numerous carbon–fluorine bonds in the molecule cause these molecules' properties and behavior to differ greatly from their nonfluorinated analogues. Since detection of PFAS with I-CIMS requires either adduct formation or proton transfer between iodide and an analyte molecule, we can use I-CIMS as a tool to better understand the fundamental properties of PFAS. Therefore, our second objective was to determine the electric field strength required to break apart PFAS-iodide adducts with voltage scanning experiments. This relates to the adduct's binding energy, which we also theoretically determined with quantum chemical calculations. From an analytical chemistry perspective, adduct binding energy offers insight into the sensitivity to a given analyte, as has been used to inform CIMS measurements of other compounds.[45,46] From a fundamental, physical chemistry perspective, measuring the binding energy between iodide and PFAS can elucidate structure-activity relationships of this poorly understood class of molecules, and help evaluate the accuracy of computationally estimated parameters.

Methods

Materials

Perfluoroalkyl sulfonic acids (PFSAs) were obtained as follows: heptadecafluorooctanesulfonic acid potassium salt (PFOS, ≥98%, Sigma-Aldrich), nonafluorobutane-1-sulfonic acid (PFBS, ≥97%, Sigma-Aldrich). perfluoroalkyl carboxylic acids (PFCAs) were obtained as follows: sodium perfluorooctanoate (PFOA, 97%, Alfa Aesar), perfluoro(2-methyl-3-oxahexanoic) acid (GenX, ≥96%, Santa Cruz Biotechnology), undecafluorohexanoic acid (PFHxA, ≥98%, TCI America), heptafluorobutyric acid (PFBA, ≥98%, TCI America). Fluorotelomer alcohols (FTOHs) were obtained as follows: 1H,1H,2H,2H-Perfluorohexanol (4:2 FTOH, Toronto Research Chemicals), 1H,1H,2H,2H-Tridecafluoro-1-octanol (6:2 FTOH, ≥98.0%, TCI America), 1H,1H,2H,2H-Perfluorodecanol (8:2 FTOH, Toronto Research Chemicals). Polyfluoro phosphate diesters (diPAPs) were obtained as follows: Bis[2-(perfluorohexyl)ethyl]phosphate (6:2 diPAP, Toronto Research Chemicals), Bis[2-(perfluorooctyl)ethyl] phosphate (8:2 diPAP, Toronto Research Chemicals). Methyl iodide (to generate reagent ion for Iodide-ToF-CIMS) was obtained from Sigma-Aldrich (99% purity).

Sample introduction techniques

Heated tube (for PFCAs)

500 ppm solutions of PFOA, PFHxA, PFBA, and GenX were made in deionized water. These solutions were aerosolized using a Collison nebulizer into a 1.5 m^3 PTFE chamber attached to a metallic frame. A scanning mobility particle sizer (SMPS) was used to monitor injection of aerosol. The outlet of the chamber was connected to a thermodenuder, with the activated carbon denuding portion removed. Therefore, it functioned as a heated tube, 2 ft long with an aerosol flow diameter of 1.5 inches. Flow inside the tube is laminar. This tube is surrounded by heating tape to maintain a temperature of approximately 200 °C. As the aerosol passes through the tube, the PFAS is vaporized, creating gas-phase PFAS. The outlet of the heated tube was connected to the iodide-CIMS, described in detail later. A schematic of the heated tube setup is found in the SI (SI Figure S1).

Diffusion tube (for FTOHs)

For more volatile PFAS, namely the fluorotelomer alcohols, heat was not necessary to create gas-phase molecules. Therefore, a diffusion tube setup was employed. 1 mL of either pure, liquid 4:2 FTOH, 6:2 FTOH, or 8:2 FTOH was added to the diffusion tube. Ultrapure nitrogen gas at a flow rate of 2000 sccm was passed through the headspace of the tube and to the inlet of the

iodide-CIMS, resulting in a steady ion signal. A schematic of the diffusion tube setup is found in the SI (SI Figure S2).

Iodide-ToF-CIMS

A long time-of-flight chemical ionization mass spectrometer (L-TOF-CIMS, Aerodyne Research Inc./Tofwerk AG) operated in negative ion mode with iodide reagent ions was used for this study.[34,47,48] Iodide reagent ions were generated by flowing methyl iodide vapor in ultrapure nitrogen through a ^{210}Po 10 mCi radioactive source. Gas-phase sampling was conducted with a sampling flow rate of 2.1 L/min and 1 Hz data acquisition using TofDaq Recorder. Initial voltage tuning was optimized manually for maximum detection of PFAS-iodide adducts; these optimal voltages are reported in the supplemental information (Table S1). Data analysis was conducted in Tofware v3.2.2.

Declustering voltage scanning

For PFCAs and FTOHs, voltage scanning experiments were performed, since these compounds readily clustered with iodide. The voltage scanning procedure was developed and described in detail by Lopez-Hilfiker et al.[46] Briefly, a script controlling the TOF Power Supply (TPS) systematically scans the voltage difference (dV) between the skimmer and entrance to the big segmented quadrupole (Figure 1, BSQ). The dV is generated by changing voltages applied to optics upstream of the skimmer while keeping those of the BSQ region the same to minimize ion mass dependent transmission efficiency changes (Figure 1). Files used for TPS scripting can be found in the supplemental info (Table S2). By increasing dV, the collisional energy of the adduct is increased, eventually leading to dissociation of the adduct into I^- and a neutral PFAS. In some cases, increasing dV also increases the signal from deprotonated PFAS anions in the mass spectrometer, which likely arise due to proton transfer with iodide.

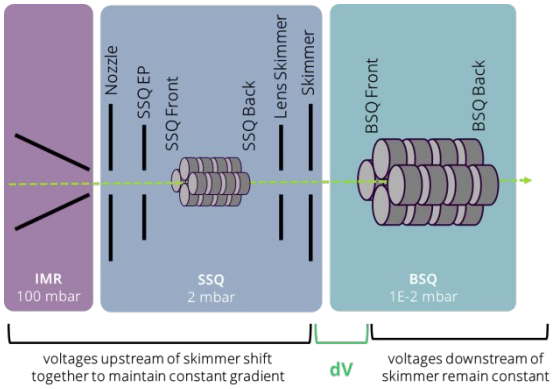

Figure 1. Schematic of the region of interest for declustering voltage scan experiments in the chemical ionization mass spectrometer (CIMS), including the ion molecule reactor (IMR), small segmented quadrupole (SSQ) and big segmented quadrupole (BSQ). The dotted green arrow represents the path an ion travels through the instrument. Note there are ion optics and voltages further downstream of the "BSQ Back" not shown here. During a declustering voltage scan, the skimmer and all voltages upstream of it are shifted incrementally towards more negative voltages, while the voltages downstream of the skimmer remain constant. This causes the voltage difference (dV) to incrementally increase while maintaining a constant overall voltage gradient, which maintains a constant mass transmission profile. As dV increases, the probability a given iodide-analyte adduct will dissociate increases.

FIGAERO inlet method (for PFSAs and diPAPs, and calibrations for all compounds except FTOHs)

PFSAs and diPAPs were not adequately volatile to be measured using the heated tube or diffusion tube setup, even at higher heated tube temperatures, or under dry conditions (using a diffusion drier and/or non-water solvent). Therefore, a Filter Inlet for Gases and AEROsols (FIGAERO) approach was used. In brief, FIGAERO employs a PTFE filter to collect aerosol, which is subsequently desorbed by a heated nitrogen flow, creating gas-phase species that can be detected with iodide-CIMS.[42] Others have developed an approach for calibrating the response of FIGAERO-CIMS by spotting known amounts of analyte onto the filter followed by a desorption procedure.[49] We adopted this approach as a proof-of-concept for the use of FIGAERO-CIMS in measuring aerosol-phase PFSAs and diPAPs. First, the PTFE filter was wetted with 5 µL methanol, followed by 5 µL of 100 ppm PFAS in aqueous solution, for a total loading of 100 ng PFAS. Then, a heating program was performed to desorb the PFAS and generate gas-phase species to be detected. Details of the heating program employed can be found in the Supplemental Information (Table S3). A summary of all analytes investigated here and pertinent information on their detection is summarized in Table S4.

Computation of Theoretical Binding Enthalpies

To complement experimental data, Gaussian 16 calculations were performed on the Extreme Science and Engineering Discovery Environment (XSEDE) cluster through the Pittsburgh Supercomputing Center's Bridges-2 resource.[50,51] These calculations were used to determine the theoretical binding enthalpies for all PFAS-iodide clusters, similar to previous work by Iyer et al.[52] First, geometry optimizations of each free PFAS were performed using the B3LYP/6-31G* level. Then, for each free molecule and its iodide adduct, a combined geometry optimization and frequency calculation were performed using the PBE functional[53] and SDD basis set. This functional and basis set were chosen because of their previous use for iodide-CIMS calculations by Iyer et al. While Iyer et al. also performed calculations at a higher order (PBE/aug-cc-pVTZ-PP) this was found to be too computationally expensive to be feasible for the PFAS of our interest.

From the output of the calculations (namely the thermal enthalpy corrected electronic energies), binding enthalpies were calculated as follows:

$$\mathrm{PFAS} + \mathrm{I}^- \rightarrow \mathrm{PFAS} - \mathrm{I}^- \mathrm{adduct} \quad (\Delta \mathrm{H}_{formation})$$

$$\Delta \mathrm{H}_{binding} = -\Delta \mathrm{H}_{formation} = \left(\Delta \mathrm{H}(\mathrm{PFAS}) + \left(\Delta \mathrm{H}(\mathrm{I}^-)\right) - \Delta \mathrm{H}(^{\mathrm{PFAS} - \mathrm{I}^- \mathrm{adduct}_{\mathrm{t}})}\right.$$

Thermal enthalpy corrected electronic energies were also used to calculate the enthalpy change during proton transfer, as follows:

$$\mathrm{PFAS} + \mathrm{I}^- + \mathrm{HI} \rightarrow [\mathrm{PFAS} - \mathrm{H}]^- \quad (\Delta \mathrm{H}_{transfer})$$

$$\Delta \mathrm{H}_{transfer} = \left(\Delta \mathrm{H}\ (\mathrm{PFAS}) + \left(\Delta \mathrm{H}\ (\mathrm{I}^-)\right) - \left(\Delta \mathrm{H}([\mathrm{PFAS} - \mathrm{H}]^-) + \Delta \mathrm{H}\ (\mathrm{HI})\right)\right.$$

Results and Discussion

Representative responses from PFAS for the three sampling approaches are shown in Figure 2. PFOA, PFHxA, PFBA, and GenX were detected primarily as iodide adducts, with a minor fraction detected as deprotonated anions. For GenX, an additional minor fraction was detected as a fragment, which has been previously observed as a result of in-source fragmentation during electrospray ionization (SI Figure S3).[54] The fluorotelomer alcohols were detected exclusively as iodide adducts, with no signal from deprotonated anions. PFOS, PFBS, and 6:2 diPAP were exclusively detected as deprotonated anions, suggesting proton exchange with iodide outcompetes adduct formation for these compounds. As expected, the heated tube and diffusion

tube methods result in steady signal of analyte, while FIGAERO does not. This is because the heated tube and diffusion tube utilize a constant flow and/or heating, while FIGAERO works by desorbing a discrete amount of analyte from a filter using a flow of heated nitrogen. Therefore, voltage scanning experiments were only conducted on PFAS that were readily detected with the heated tube or diffusion tube methods. A summary of the advantages and disadvantages of each method are presented in Table 1.

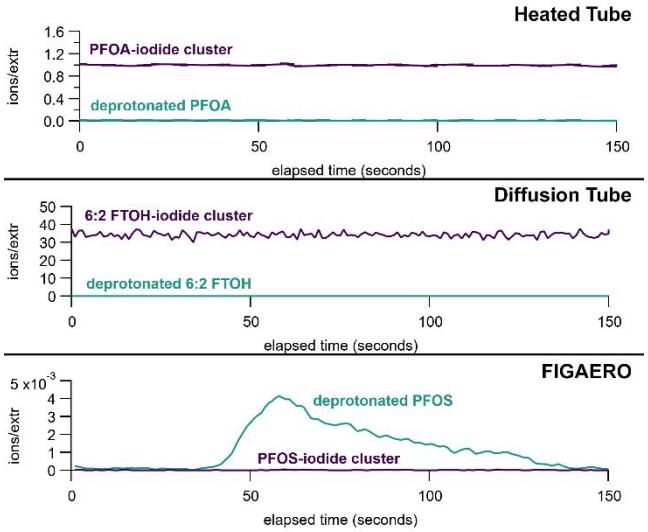

Figure 2. Comparison of typical signals of PFAS from the three sample introduction techniques used in this work. Top: PFOA signal from heated tube, Middle: 6:2 FTOH signal from diffusion tube, Bottom: PFOS signal from FIGAERO.

Table 1. Comparison of the three sample introduction methods used in this work.

Method	**Advantages**	**Disadvantages**
Heated tube	Provides very steady signal, ideal for voltage scanning	Even at upper limit of heating tape, low volatility PFAS cannot be detected
Diffusion tube	Provides very steady signal, ideal for voltage scanning	Only works for very volatile PFAS (fluorotelomer alcohols)
FIGAERO	Works for lower volatility compounds, can give insight into trends of volatility for compounds, can be used for calibration	Yields thermograms rather than steady, constant signals, so not ideal for voltage scanning

Results of voltage scanning experiments show a trend with chain length and functional group type (Figure 3). As expected, all adducts follow a sigmoidal response to the voltage difference between the Skimmer and front of the BSQ (dV). We define the point at which 50% of the initial adduct remains as dV_{50} and use this value to characterize the binding energy of each adduct. It is important to note that the signal from the PFOA/iodide and PFHxA adducts initially increased as dV increased, followed by the expected decay. This can be attributed to the fact that dV actually does play a small role in ion transmission. Large ions require a high dV to be transmitted efficiently though the BSQ. If the initial conditions were more optimized for PFOA and PFHxA transmission, this behavior would have not been observed. However, so that all of the data collected here was directly comparable, we used the same initial voltage tuning for all compounds.

We observed that PFCAs had higher dV_{50} values (and thus stronger binding to iodide) than FTOHs (Table 2). Furthermore, within each class, a chain length dependence on dV_{50} was observed, with longer linear chain compounds having stronger binding with iodide. GenX, the only branched PFCA studied, had a lower dV_{50} than PFHxA, a linear PFCA with the same number of carbons. The finding that PFCAs tend to form stronger adducts with iodide than FTOHs is likely due to higher partial positive charge on the proton interacting with the iodide. In the case of PFCAs, the other oxygens on the carbon containing the alcohol group and the fluorines on the carbon alpha to the carbonyl draw electron density away, making the proton more positively charged. By contrast, the alcohol group in FTOHs is several carbons away from any fluorine atoms, meaning that the proton has less partial negative charge. This is corroborated by the acidity of PFCAs as compared to analogous FTOHs.

The observed positive correlation between linear chain length and adduct strength is likely due to a similar phenomenon. Calculated proton transfer enthalpies within the PFCA group and the FTOH group increase as linear chain length decreases. This indicates that longer chain compounds are more acidic, which by extension indicates that the proton has an especially high partial positive charge. This would increase the binding energy between the proton and the iodide, creating a higher adduct strength. This trend does not hold for GenX, the only branched molecule studied. GenX had the lowest observed dV50 of the PFCAs, but also the lowest enthalpy of proton transfer. It is possible that the relatively weak adduct between GenX and iodide is due to sterics rather than charge distribution.

Table 2. Comparison of experimentally determined dV_{50} values (iodide adduct binding energy) and computationally determined binding enthalpy values for PFAS studied. Binding enthalpies were calculated in Gaussian16 at the PBE level of theory with the SDD basis set.

Compound	Class	Formula	enthalpy of adduct formation (kcal/mol)	enthalpy of proton transfer (kcal/mol)	Measured dV_{50} (volts)
GenX	PFCA	$C_6HF_{11}O_3$	-27.94	0.01	8.44
PFBA		$C_4HF_7O_2$	-27.56	4.43	8.76
PFHxA		$C_6HF_{11}O_2$	-27.82	3.16	12.3
PFOA		$C_8HF_{15}O_2$	-27.96	2.72	13.0
4:2 FTOH	FTOH	$C_6H_5F_9O$	-21.8	54.36	6.55
6:2 FTOH		$C_8H_5F_{13}O$	-19.39	50.29	6.75
8:2 FTOH		$C_{10}H_5F_{17}O$	-22.33	47.39	7.70
PFBS	PFSA	$C_4HF_9O_3S$	-32.94	-5.13	N/A
PFOS		$C_8HF_{17}O_3S$	-32.46	-4.54	N/A
6:2 diPAP	diPAP	$C_{16}H_9F_{26}O_4P$	-33.58	0.06	N/A
8:2 diPAP		$C_{20}H_9F_{34}O_4P$	-33.65	-0.05	N/A

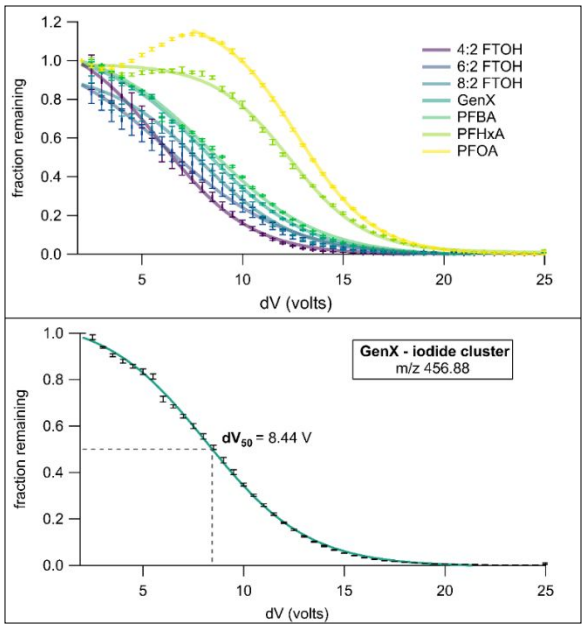

Figure 3. Experimentally determined dV_{50} values for PFAS-iodide adducts. Top: declustering scans of PFAS-iodide adducts studied. Error bars represent standard error of three replicate measurements. Within each class of PFAS (FTOH and PFCA), binding energy increases with increasing linear chain length. Bottom: Representative example of sigmoidal fit performed on experimental declustering scan data for GenX. Average of triplicate measurements and standard error are shown in black, and the sigmoidal fit is shown in teal.

Previously, Lopez-Hilfiker et al. utilized a declustering voltage scanning procedure to constrain the sensitivity of iodide CIMS to a variety of atmospherically relevant species, especially gas-phase secondary organic aerosol (SOA) precursors.[46] Since previous work focused largely on SOA, there was little overlap in the analytes measured by Lopez-Hilfiker et al. and those measured by us in this work. Thankfully, due to high sensitivity of iodide-CIMS, nitric acid is measurable even at low, ambient levels. Therefore, even though we did not intend to measure nitric acid-iodide clusters, they were still present in measurable levels in our experiments, allowing us to collect adduct declustering scans for nitric acid alongside each PFAS experiment. (Figure 4). This served two purposes: 1) it enables a quality check of the consistency of data collection within our study and 2) it enables comparison to previous work. Regarding the former, we observed a consistent declustering scan profile and dV_{50} values for nitric acid across multiple days and various PFAS introduction techniques. This bodes well for direct comparison of the voltage scans of various PFAS (which were conducted on different days, with different introduction techniques) in this work. As for the latter, all compounds studied here have quite strong binding energies, relative to compounds typically detected in oxidized secondary organic aerosol (SOA) investigated

in previous work. It is worthy to note that both this work and previous work characterized nitric acid, yielding different fit dV_{50} values (5.50 V in previous work, 7.74 V in this work). This is likely due to differences between experimental conditions and voltage tuning of the CIMS.

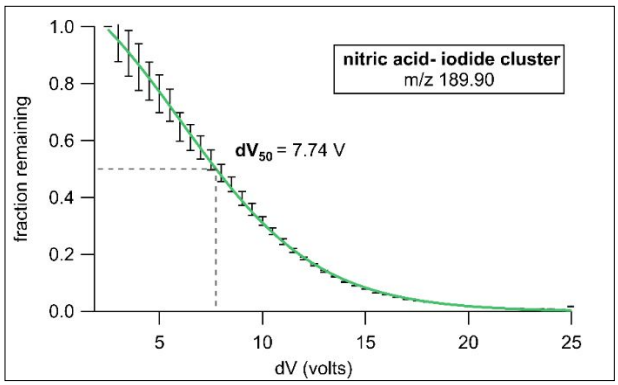

Figure 4. Sigmoidal fit performed on experimental declustering scan data for nitric acid. The average of 21 measurements spanning the duration of the study and standard error are shown in black, and the sigmoidal fit is shown in green.

Plotting measured dV_{50} values versus calculated binding energies resulted in two distinct groups (Figure 5). The first group is comprised of FTOHs and nitric acid, for which there is a reasonably linear correlation between dV_{50} and binding energy (R^2 = 0.64). The second group is comprised of PFCAs, for which there appears to be no correlation between calculated binding enthalpy and measured dV_{50}. Together, this indicates that binding enthalpy may have an upper limit of usefulness as a metric for adduct transmission through the ion optics of the CIMS. The relationship between calculated binding enthalpy and measured dV_{50} may be especially problematic for PFCAs, since PFOA and PFHxA mass transmission shifted with dV. Finally, it's possible the level of theory used in our computations was not sufficient to capture the behavior of PFAS clustering with iodide.

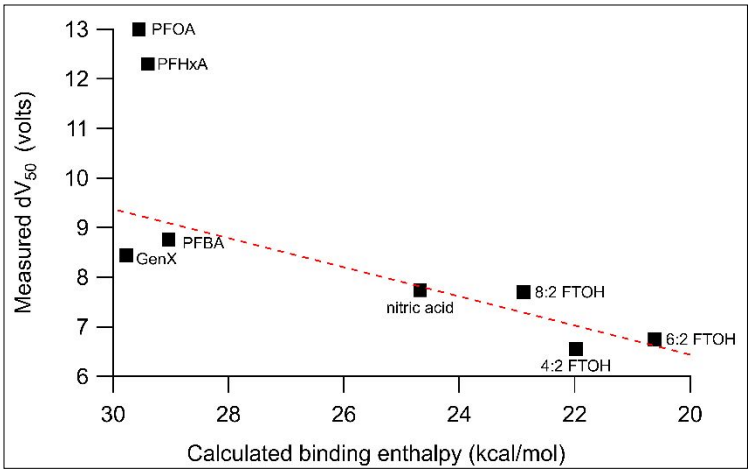

Figure 5. Relationship between calculated binding energy and measured dV_{50} for PFAS that formed clusters with iodide reagent ions and for nitric acid. The linear fit shown is just for nitric acid and the FTOHs, extrapolated to show that it's a poor fit for the PFCAs.

Another interesting finding from computations is that the calculated binding energies for the PFAS that we observe do not cluster with iodide (PFBS, PFOS, 6:2 diPAP, 8:2 diPAP) are even higher than PFCAs, which strongly bind to iodide (Table 1). It is important to note that binding enthalpy is merely an indication of the stability of an adduct after it has been formed, not necessarily the likelihood of that adduct forming via a successful collision in the IMR in the first place. Since we do not observe PFSA or diPAP adducts with iodide, but computations indicate they would be strongly bound and thus not dissociate under the voltage conditions used here, then it follows that PFSAs and diPAPs are not forming adducts with iodide in the IMR. FIGAERO thermograms collected show that PFSAs and diPAPs are actually detected primarily as their deprotonated anions, indicating proton transfer with iodide occurs preferentially over adduct formation (Figure 6). This is corroborated by the very low (and often negative) proton transfer enthalpies we calculated for PFSAs and diPAPs. Proton transfer with iodide is generally ignored for atmospheric measurements, since it is assumed that the only atmospherically relevant compound capable of proton transfer with iodide is sulfuric acid.34 However, many PFAS species have adequately low pKa values to facilitate proton transfer to iodide, meaning these species may be more easily detected as their deprotonated anions. PFOA – which has a higher pKa than its analogous PFSA, PFOS – undergoes proton transfer to some extent, but not enough to outcompete iodide adduct formation (Figure 6). As interest in PFAS detection via CIMS increases, we must be careful to not extend our assumptions about the behavior of conventionally studied atmospheric compounds to PFAS without careful consideration of the validity of these assumptions. This is especially

important given that PFAS have many unique physical properties due to the extensive fluorination of the carbon backbone.

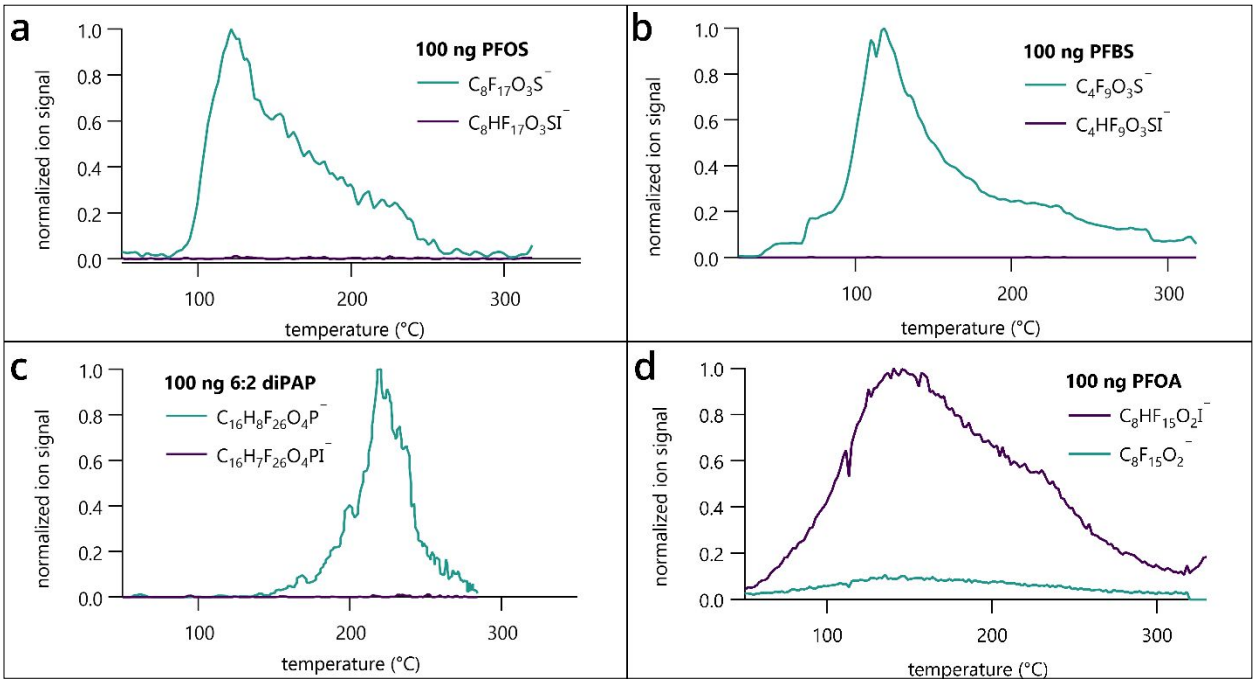

Figure 6. Normalized FIGAERO thermograms of aqueous solutions containing 100 ng of a) PFOS, b) PFBS, c) 6 :2 diPAP, and d) PFOA. For all plots, the purple trace represents the iodide-PFAS cluster, while the teal trace represents a deprotonated PFAS anion.

FIGAERO thermograms also enabled calibration of the instrument response to PFCAs, PFSAs, and diPAPs (Figure 6). By integrating the ion signal measured over each thermogram and dividing by the mass spotted on the filter, we can calculate the expected ion signal per nanogram of PFAS. Our method is most sensitive to PFOA, with an expected signal of 6.0 x 10^4 ions per nanogram. PFBS and PFOS are detected with a factor of 10 lower sensitivities at 5.9 x 10^3 and 1.9 x 10^3 ions/ng, respectively. Our method is least sensitive to 6:2 diPAP with 4.0 x 10^2 ions/ng. Furthermore, since FIGAERO thermograms show the temperature at which analyte signal is maximized (T_{max}), these plots can be used to understand the effective volatility of the PFAS studied. PFOA, PFOS, and PFBS exhibited similar T_{max} values (140 °C, 123 °C, and 117 °C, respectively), while 6:2 diPAP is less volatile (218 °C). This is an expected result based on the structures of these compounds – PFOA, PFBS and PFOS are structurally similar, while 6:2 diPAP has two long fluorinated chains as opposed to just one. All compounds were fully desorbed by the FIGAERO temperature program, which indicates they are sufficiently volatile to be detected quantitatively in the aerosol phase by FIGAERO-Iodide-ToF-CIMS. Finally, it is possible that some

fraction of PFAS is scavenged via sorption to the PTFE filter in the FIGAERO.[55] Therefore, these instrument responses should be considered upper bounds of sensitivity. Investigating alternate filters for PFAS detection via FIGAERO CIMS is an opportunity for future work.

Conclusions

While it is likely that incineration of waste, manufacture of products containing PFAS, and sea spray aerosol emissions result in emission of these compounds to the atmosphere, these processes are not well understood.[56] Due to the persistence and toxicity of PFAS, these inputs have serious implications for human health and the global distribution of PFAS contamination. Online measurements, such as CIMS, provide specific highly time resolved measurements at the molecular level that don't suffer from the same sampling artefacts and biases as offline methods. Previous work by Riedel et al. using iodide ToF-CIMS was only successful in measuring PFCAs and FTOHs. While these compounds are atmospherically relevant, there are many other PFAS that were not able to be measured, including PFSAs and diPAPs. The authors of previous work attributed this either to insufficient volatility or lack of iodide-adduct formation. Our work suggests the latter is true – PFSAs and diPAPs do not cluster with iodide, but this does not preclude detection, since they still form ions through proton transfer. Given that PFSAs and diPAPs were not successfully measured with the heated tube method, and only produced measurable vapor under FIGAERO conditions, it seems likely that the low volatility of PFSAs and diPAPs are the cause for measurement challenges experienced by Riedel et al. While those authors point out that PFSAs and diPAPs are routinely measured in the condensed phase via LC-MS (an offline technique), we propose that an online method using FIGAERO is a promising approach for measurement of these less volatile PFAS, so long as they are monitored at the m/z corresponding to $[M\text{-}H]^-$ and not $[M+I]^-$.

Ample opportunity for future work to further evaluate the use of CIMS for PFAS detection and quantification remains. First, this study only investigated a fraction of the myriad PFAS present in the environment today, so future work could investigate other PFAS. Furthermore, additional reagent ion chemistries (e.g. acetate, nitrate) would be worth studying to determine if those reagent ions cluster in a similar fashion with PFAS and if they are more promising for field deployment. For example, iodide detection is very sensitive to changes in relative humidity, while acetate is relatively less so.[57] The limits of detection and sensitivity/calibration factors should also

be determined, though this requires generating a well-known concentration of the gas-phase PFAS substrate.

Acknowledgements

The authors would like to thank Hyung Kim, Fangyong Yan, Theo Kurtén, Siddharth Iyer, and Megan Van Horn for their assistance with the computational aspects of this work. This work used the Extreme Science and Engineering Discovery Environment (XSEDE), which is supported by National Science Foundation grant number ACI-1548562. More specifically, the Bridges-2 system at the Pittsburgh Supercomputing Center (PSC) is supported by NSF Grant No. ACI-1928147 and was used through allocation TG-CHE220024. The LToF-CIMS used in this work was acquired through the National Science Foundation Major Research Instrumentation Program award number AGS-1531284.

References

1 Z. Wang, J. C. Dewitt, C. P. Higgins and I. T. Cousins, A Never-Ending Story of Per- and Polyfluoroalkyl Substances (PFASs)?, *Environ. Sci. Technol.*, 2017, **51**, 2508–2518.

2 I. T. Cousins, R. Vestergren, Z. Wang, M. Scheringer and M. S. McLachlan, The precautionary principle and chemicals management: The example of perfluoroalkyl acids in groundwater, *Environ. Int.*, 2016, **94**, 331–340.

3 E. L. D'Ambro, H. O. T. Pye, J. O. Bash, J. Bowyer, C. Allen, C. Efstathiou, R. C. Gilliam, L. Reynolds, K. Talgo and B. N. Murphy, Characterizing the Air Emissions, Transport, and Deposition of Per- And Polyfluoroalkyl Substances from a Fluoropolymer Manufacturing Facility, *Environ. Sci. Technol.*, 2021, **55**, 862–870.

4 Y. Tian, Y. Yao, S. Chang, Z. Zhao, Y. Zhao, X. Yuan, F. Wu and H. Sun, Occurrence and Phase Distribution of Neutral and Ionizable Per- and Polyfluoroalkyl Substances (PFASs) in the Atmosphere and Plant Leaves around Landfills: A Case Study in Tianjin, China, *Environ. Sci. Technol.*, 2018, **52**, 1301–1310.

5 C. A. Barton, L. E. Butler, C. J. Zarzecki, J. Flaherty and M. Kaiser, Characterizing perfluorooctanoate in ambient air near the fence line of a manufacturing facility: comparing modeled and monitored values, *J. Air Waste Manag. Assoc.*, 2006, **56**, 48–55.

6 L. Ahrens, M. Shoeib, T. Harner, S. C. Lee, R. Guo and E. J. Reiner, Wastewater treatment plant and landfills as sources of polyfluoroalkyl compounds to the atmosphere, *Environ. Sci. Technol.*, 2011, **45**, 8098–8105.

7 B. Wang, Y. Yao, H. Chen, S. Chang, Y. Tian and H. Sun, Per- and polyfluoroalkyl substances and the contribution of unknown precursors and short-chain (C2–C3) perfluoroalkyl carboxylic acids at solid waste disposal facilities, *Sci. Total Environ.*, 2020, **705**, 135832.

8 I. Weinberg, A. Dreyer and R. Ebinghaus, Landfills as sources of polyfluorinated compounds, polybrominated diphenyl ethers and musk fragrances to ambient air, *Atmos.*

Environ., 2011, **45**, 935–941.

9 J. Roth, I. Abusallout, T. Hill, C. Holton, U. Thapa and D. Hanigan, Release of Volatile Per-and Polyfluoroalkyl Substances from Aqueous Film-Forming Foam, *Environ. Sci. Technol. Lett.*, 2020, **7**, 164–170.

10 K. Winkens, J. Koponen, J. Schuster, M. Shoeib, R. Vestergren, U. Berger, A. M. Karvonen, J. Pekkanen, H. Kiviranta and I. T. Cousins, Perfluoroalkyl acids and their precursors in indoor air sampled in children's bedrooms, *Environ. Pollut.*, 2017, **222**, 423–432.

11 M. E. Morales-Mcdevitt, J. Becanova, A. Blum, T. A. Bruton, S. Vojta, M. Woodward and R. Lohmann, The Air That We Breathe: Neutral and Volatile PFAS in Indoor Air, *Environ. Sci. Technol. Lett.*, , DOI:10.1021/acs.estlett.1c00481.

12 J. Zhou, K. Baumann, N. Chang, G. Morrison, W. Bodnar, Z. Zhang, J. M. Atkin, J. D. Surratt and B. J. Turpin, Per- and polyfluoroalkyl substances (PFASs) in airborne particulate matter (PM2.0) emitted during floor waxing: A pilot study, *Atmos. Environ.*, 2022, **268**, 118845.

13 J. W. Washington, C. G. Rosal, J. P. McCord, M. J. Strynar, A. B. Lindstrom, E. L. Bergman, S. M. Goodrow, H. K. Tadesse, A. N. Pilant, B. J. Washington, M. J. Davis, B. G. Stuart and T. M. Jenkins, Nontargeted mass-spectral detection of chloroperfluoropolyether carboxylates in New Jersey soils, *Science (80-.).*, 2020, **368**, 1103–1107.

14 H. M. Pickard, A. S. Criscitiello, D. Persaud, C. Spencer, D. C. G. Muir, I. Lehnherr, M. J. Sharp, A. O. De Silva and C. J. Young, Ice Core Record of Persistent Short-Chain Fluorinated Alkyl Acids: Evidence of the Impact From Global Environmental Regulations, *Geophys. Res. Lett.*, , DOI:10.1029/2020GL087535.

15 T. Schroeder, D. Bond and J. Foley, PFAS soil and groundwater contamination via industrial airborne emission and land deposition in SW Vermont and Eastern New York State, USA, *Environ. Sci. Process. Impacts*, 2021, **23**, 291–301.

16 Y. Wu, K. Romanak, T. Bruton, A. Blum and M. Venier, Per- and polyfluoroalkyl substances in paired dust and carpets from childcare centers, *Chemosphere*, 2020, **251**, 126771.

17 A. S. Young, E. H. Sparer-Fine, H. M. Pickard, E. M. Sunderland, G. F. Peaslee and J. G. Allen, Per- and polyfluoroalkyl substances (PFAS) and total fluorine in fire station dust, *J. Expo. Sci. Environ. Epidemiol.*, 2021, **31**, 930–942.

18 L. Ahrens, M. Shoeib, T. Harner, D. A. Lane, R. Guo and E. J. Reiner, Comparison of annular diffusion denuder and high volume air samplers for measuring per- and polyfluoroalkyl substances in the atmosphere, *Anal. Chem.*, 2011, **83**, 9622–9628.

19 H. P. H. Arp and K. U. Goss, Gas/particle partitioning behavior of perfluorocarboxylic acids with terrestrial aerosols, *Environ. Sci. Technol.*, 2009, **43**, 8542–8547.

20 N. L. Stock, F. K. Lau, D. A. Ellis, J. W. Martin, D. C. G. Muir and S. A. Mabury, Polyfluorinated Telomer Alcohols and Sulfonamides in the North American Troposphere, *Environ. Sci. Technol.*, 2004, **38**, 991–996.

21 M. Shoeib, T. Harner, G. M. Webster and S. C. Lee, Indoor sources of poly- and

perfluorinated compounds (PFCS) in Vancouver, Canada: Implications for human exposure, *Environ. Sci. Technol.*, 2011, **45**, 7999–8005.

22 D. A. Ellis, J. W. Martin, A. O. De Silva, S. A. Mabury, M. D. Hurley, M. P. Sulbaek Andersen and T. J. Wallington, Degradation of fluorotelomer alcohols: A likely atmospheric source of perfluorinated carboxylic acids, *Environ. Sci. Technol.*, 2004, **38**, 3316–3321.

23 C. M. Butt, D. C. G. Muir and S. A. Mabury, Biotransformation pathways of fluorotelomer-based polyfluoroalkyl substances: A review, *Environ. Toxicol. Chem.*, 2014, **33**, 243–267.

24 S. A. Styler, A. L. Myers and D. J. Donaldson, Heterogeneous Photooxidation of Fluorotelomer Alcohols: A New Source of Aerosol-Phase Perfluorinated Carboxylic Acids, , DOI:10.1021/es4011509.

25 J. W. Martin, B. J. Asher, S. Beesoon, J. P. Benskin and M. S. Ross, PFOS or PreFOS? Are perfluorooctane sulfonate precursors (PreFOS) important determinants of human and environmental perfluorooctane sulfonate (PFOS) exposure?, *J. Environ. Monit.*, 2010, **12**, 1979–2004.

26 S. Fang, C. Li, L. Zhu, H. Yin, Y. Yang, Z. Ye and I. T. Cousins, Spatiotemporal distribution and isomer profiles of perfluoroalkyl acids in airborne particulate matter in Chengdu City, China, *Sci. Total Environ.*, 2019, **689**, 1235–1243.

27 B. Sha, J. H. Johansson, P. Tunved, P. Bohlin-Nizzetto, I. T. Cousins and M. E. Salter, Sea Spray Aerosol (SSA) as a Source of Perfluoroalkyl Acids (PFAAs) to the Atmosphere: Field Evidence from Long-Term Air Monitoring, *Environ. Sci. Technol.*, 2022, **56**, 228–238.

28 A. O. De Silva, C. N. Allard, C. Spencer, G. M. Webster and M. Shoeib, Phosphorus-containing fluorinated organics: Polyfluoroalkyl phosphoric acid diesters (diPAPs), perfluorophosphonates (PFPAs), and perfluorophosphinates (PFPIAs) in residential indoor dust, *Environ. Sci. Technol.*, 2012, **46**, 12575–12582.

29 S. M. Hall, S. Patton, M. Petreas, S. Zhang, A. L. Phillips, K. Hoffman and H. M. Stapleton, Per- And Polyfluoroalkyl Substances in Dust Collected from Residential Homes and Fire Stations in North America, *Environ. Sci. Technol.*, 2020, **54**, 14558–14567.

30 K. Winkens, G. Giovanoulis, J. Koponen, R. Vestergren, U. Berger, A. M. Karvonen, J. Pekkanen, H. Kiviranta and I. T. Cousins, Perfluoroalkyl acids and their precursors in floor dust of children's bedrooms – Implications for indoor exposure, *Environ. Int.*, 2018, **119**, 493–502.

31 F. Xu, D. Chen, X. Liu, Q. Guan, H. Tan, D. Zhou, Y. Shi, J. Liu and Y. Hu, Emerging and legacy per- and polyfluoroalkyl substances in house dust from South China: Contamination status and human exposure assessment, *Environ. Res.*, 2021, **192**, 110243.

32 T. Savvaides, J. P. Koelmel, Y. Zhou, E. Z. Lin, P. Stelben, J. J. Aristizabal-Henao, J. A. Bowden and K. J. Godri Pollitt, Prevalence and Implications of Per- and Polyfluoroalkyl Substances (PFAS) in Settled Dust, *Curr. Environ. Heal. Reports*, 2021, **8**, 323–335.

33 Y. Yao, Y. Meng and H. Sun, Heterogeneous photooxidation of 6:2 polyfluoroalkyl phosphoric acid diester on dust mineral components under simulated sunlight and the influence of relative humidity and oxygen, *Chemosphere*, 2021, **281**, 130713.

34 B. H. Lee, F. D. Lopez-Hilfiker, C. Mohr, T. Kurtén, D. R. Worsnop and J. A. Thornton, An iodide-adduct high-resolution time-of-flight chemical-ionization mass spectrometer: Application to atmospheric inorganic and organic compounds, *Environ. Sci. Technol.*, 2014, **48**, 6309–6317.

35 Y. Liu, L. A. D'Agostino, G. Qu, G. Jiang and J. W. Martin, High-resolution mass spectrometry (HRMS) methods for nontarget discovery and characterization of poly- and per-fluoroalkyl substances (PFASs) in environmental and human samples, *TrAC - Trends Anal. Chem.*, 2019, **121**, 115420.

36 P. Jacob, K. A. Barzen-Hanson and D. E. Helbling, Target and nontarget analysis of per- And polyfluoralkyl substances in wastewater from electronics fabrication facilities, *Environ. Sci. Technol.*, 2021, **55**, 2346–2356.

37 N. Yu, H. Wen, X. Wang, E. Yamazaki, S. Taniyasu, N. Yamashita, H. Yu and S. Wei, Nontarget Discovery of Per- and Polyfluoroalkyl Substances in Atmospheric Particulate Matter and Gaseous Phase Using Cryogenic Air Sampler, *Environ. Sci. & Technol.*, 2020, **0**, 3103–3113.

38 K. A. Barzen-Hanson, S. C. Roberts, S. Choyke, K. Oetjen, A. McAlees, N. Riddell, R. McCrindle, P. L. Ferguson, C. P. Higgins and J. A. Field, Discovery of 40 Classes of Per- and Polyfluoroalkyl Substances in Historical Aqueous Film-Forming Foams (AFFFs) and AFFF-Impacted Groundwater, *Environ. Sci. Technol.*, 2017, **51**, 2047–2057.

39 E. F. Houtz, C. P. Higgins, J. A. Field and D. L. Sedlak, Persistence of perfluoroalkyl acid precursors in AFFF-impacted groundwater and soil, *Environ. Sci. Technol.*, 2013, **47**, 8187–8195.

40 C. A. McDonough, S. Choyke, K. E. Barton, S. Mass, A. P. Starling, J. L. Adgate and C. P. Higgins, Unsaturated PFOS and Other PFASs in Human Serum and Drinking Water from an AFFF-Impacted Community, *Environ. Sci. Technol.*, 2021, **55**, 8139–8148.

41 T. P. Riedel, J. Lang, M. J. Strynar, A. B. Lindstrom and J. H. Offenberg, Gas-Phase Detection of Fluorotelomer Alcohols and Other Oxygenated PFAS by Chemical Ionization Mass Spectrometry, *Environ. Sci. Technol. Lett.*, 2019, acs.estlett.9b00196.

42 F. D. Lopez-Hilfiker, C. Mohr, M. Ehn, F. Rubach, E. Kleist, J. Wildt, T. F. Mentel, A. Lutz, M. Hallquist, D. Worsnop and J. A. Thornton, A novel method for online analysis of gas and particle composition: Description and evaluation of a filter inlet for gases and AEROsols (FIGAERO), *Atmos. Meas. Tech.*, 2014, **7**, 983–1001.

43 C. Mohr, F. D. Lopez-Hilfiker, P. Zotter, A. S. H. Prévoît, L. Xu, N. L. Ng, S. C. Herndon, L. R. Williams, J. P. Franklin, M. S. Zahniser, D. R. Worsnop, W. B. Knighton, A. C. Aiken, K. J. Gorkowski, M. K. Dubey, J. D. Allan and J. A. Thornton, Contribution of nitrated phenols to wood burning brown carbon light absorption in detling, united kingdom during winter time, *Environ. Sci. Technol.*, 2013, **47**, 6316–6324.

44 J. A. Thornton, C. Mohr, S. Schobesberger, E. L. D'Ambro, B. H. Lee and F. D. Lopez-Hilfiker, Evaluating Organic Aerosol Sources and Evolution with a Combined Molecular Composition and Volatility Framework Using the Filter Inlet for Gases and Aerosols (FIGAERO), *Acc. Chem. Res.*, 2020, **53**, 1415–1426.

45 A. Zaytsev, M. Breitenlechner, A. R. Koss, C. Y. Lim, J. C. Rowe, J. H. Kroll and F. N. Keutsch, Using collision-induced dissociation to constrain sensitivity of ammonia chemical

ionization mass spectrometry (NH₄⁺-CIMS) to oxygenated volatile organic compounds, *Atmos. Meas. Tech. Discuss.*, 2018, 1–20.

46 F. D. Lopez-Hilfiker, S. Iyer, C. Mohr, B. H. Lee, E. L. D'ambro, T. Kurtén and J. A. Thornton, Constraining the sensitivity of iodide adduct chemical ionization mass spectrometry to multifunctional organic molecules using the collision limit and thermodynamic stability of iodide ion adducts, *Atmos. Meas. Tech.*, 2016, **9**, 1505–1512.

47 D. Aljawhary, A. K. Y. Lee and J. P. D. Abbatt, High-resolution chemical ionization mass spectrometry (ToF-CIMS): Application to study SOA composition and processing, *Atmos. Meas. Tech.*, 2013, **6**, 3211–3224.

48 J. P. Kercher, T. P. Riedel and J. A. Thornton, Chlorine activation by N2O5: simultaneous, in situ detection of ClNO2 and N2O5 by chemical ionization mass spectrometry, *Atmos. Meas. Tech.*, 2009, **2**, 193–204.

49 A. Ylisirniö, L. M. F. Barreira, I. Pullinen, A. Buchholz, J. Jayne, J. E. Krechmer, D. R. Worsnop, A. Virtanen and S. Schobesberger, On the calibration of FIGAERO-ToF-CIMS: Importance and impact of calibrant delivery for the particle-phase calibration, *Atmos. Meas. Tech.*, 2021, **14**, 355–367.

50 M. J. Frisch, G. W. Trucks, H. B. Schlegel, G. E. Scuseria, M. a. Robb, J. R. Cheeseman, G. Scalmani, V. Barone, G. a. Petersson, H. Nakatsuji, X. Li, M. Caricato, a. V. Marenich, J. Bloino, B. G. Janesko, R. Gomperts, B. Mennucci, H. P. Hratchian, J. V. Ortiz, a. F. Izmaylov, J. L. Sonnenberg, Williams, F. Ding, F. Lipparini, F. Egidi, J. Goings, B. Peng, A. Petrone, T. Henderson, D. Ranasinghe, V. G. Zakrzewski, J. Gao, N. Rega, G. Zheng, W. Liang, M. Hada, M. Ehara, K. Toyota, R. Fukuda, J. Hasegawa, M. Ishida, T. Nakajima, Y. Honda, O. Kitao, H. Nakai, T. Vreven, K. Throssell, J. a. Montgomery Jr., J. E. Peralta, F. Ogliaro, M. J. Bearpark, J. J. Heyd, E. N. Brothers, K. N. Kudin, V. N. Staroverov, T. a. Keith, R. Kobayashi, J. Normand, K. Raghavachari, a. P. Rendell, J. C. Burant, S. S. Iyengar, J. Tomasi, M. Cossi, J. M. Millam, M. Klene, C. Adamo, R. Cammi, J. W. Ochterski, R. L. Martin, K. Morokuma, O. Farkas, J. B. Foresman and D. J. Fox, 2016.

51 J. Towns, T. Cockerill, M. Dahan, I. Foster, K. Gaither, A. Grimshaw, V. Hazlewood, S. Lathrop, D. Lifka, G. D. Peterson, R. Roskies, J. R. Scott and N. Wilkens-Diehr, XSEDE: Accelerating Scientific Discovery, *Comput. Sci. Eng.*, 2014, **16**, 62–74.

52 S. Iyer, F. Lopez-Hilfiker, B. H. Lee, J. A. Thornton and T. Kurtén, Modeling the Detection of Organic and Inorganic Compounds Using Iodide-Based Chemical Ionization, *J. Phys. Chem. A*, 2016, **120**, 576–587.

53 J. P. Perdew, K. Burke and M. Ernzerhof, Generalized gradient approximation made simple, *Phys. Rev. Lett.*, 1996, **77**, 3865–3868.

54 D. Vughs, K. A. Baken, M. M. L. Dingemans and P. De Voogt, The determination of two emerging perfluoroalkyl substances and related halogenated sulfonic acids and their significance for the drinking water supply chain, *Environ. Sci. Process. Impacts*, 2019, **21**, 1899–1907.

55 B. Chandramouli, J. P. Benskin, M. C. Hamilton and J. R. Cosgrove, Sorption of per- and polyfluoroalkyl substances (PFASs) on filter media: Implications for phase partitioning studies, *Environ. Toxicol. Chem.*, 2015, **34**, 30–36.

56 J. Wang, Z. Lin, X. He, M. Song, P. Westerhoff, K. Doudrick and D. Hanigan, Critical Review of Thermal Decomposition of Per- and Polyfluoroalkyl Substances: Mechanisms and Implications for Thermal Treatment Processes, *Environ. Sci. & Technol.*, 2022, **56**, 5355–5370.

57 P. Brophy and D. K. Farmer, A switchable reagent ion high resolution time-of-flight chemical ionization mass spectrometer for real-time measurement of gas phase oxidized species: characterization from the 2013 southern oxidant and aerosol study, *Atmos. Meas. Tech.*, 2015, **8**, 2945–2959.